Understanding the association between climate variability and the Nile's water level fluctuations and water storage changes during 1992-2016

M. Khaki[a,b,1], J. Awange[a], E. Forootan[c], M. Kuhn[a]

[a]*School of Earth and Planetary Sciences, Discipline of Spatial Sciences, Curtin University, Perth, Australia.*

[b]*School of Engineering, University of Newcastle, Callaghan, New South Wales, Australia.*

[c]*School of Earth and Ocean Sciences, Cardiff University, Cardiff, UK.*

Abstract

With the construction of the largest dam in Africa, the Grand Ethiopian Renaissance Dam (GERD) along the Blue Nile, the Nile is back in the news. This, combined with Bujagali dam on the White Nile are expected to bring ramification to the downstream countries. A comprehensive analysis of the Nile's waters (surface, soil moisture and groundwater) is, therefore, essential to inform its management. Owing to its shear size, however, obtaining in-situ data from "boots on the ground" is practically impossible, paving way to the use of satellite remotely sensed and models' products. The present study employs multi-mission satellites and surface models' products to provide, for the first time, a comprehensive analysis of the changes in Nile's stored waters' compartments; surface, soil moisture and groundwater, and their association to climate variability (El Niño Southern Oscillation (ENSO) and Indian Ocean Dipole (IOD)) over the period 1992-2016. In this regard, remotely sensed altimetry data from TOPEX/Poseidon (T/P), Jason-1, and Jason-2 satellites along with the Gravity Recovery And Climate Experiment (GRACE) mission, and the Tropical Rainfall Measuring Mission Project (TRMM) rainfall products are applied to analyze the compartmental changes over the Nile River Basin (NRB). This is achieved through the creation of 62 virtual gauge stations distributed throughout the Nile River that generate water levels, which are used to compute surface water storage changes. Using GRACE total water storage (TWS), soil moisture data from multi-models based on the Triple Collocation Analysis (TCA) method, and altimetry derived surface water storage, Nile basin's groundwater variations are estimated. The impacts of climate variability on the compartmental changes are examined using TRMM precipitation and large-scale ocean-atmosphere ENSO and IOD indices. The results indicate a strong correlation between the river level varia-

Email address: Mehdi.Khaki@postgrad.curtin.edu.au (M. Khaki)

tions and precipitation changes in the central part of the basin (0.77 on average) in comparison to the northern (0.64 on average) and southern parts (0.72 on average). Larger water storages and rainfall variations are observed in the Upper Nile in contrast to the Lower Nile. A negative groundwater trend is also found over the Lower Nile, which could be attributed to a significantly lower amount of rainfall in the last decade and extensive irrigation over the region.

Keywords: Climate variability, Satellite altimetry, River Nile, Groundwater, Water level, GRACE .

1. Introduction

The Nile River, arguably the longest river in the world (6800 km), has a major impact on the livelihood of over 300 million people of 11 countries within the region. This population is expected to double in the next twenty-five years (Nunzio, 2013) thereby putting extreme pressure on its water resources. Already now, this pressure is building up with the upper stream countries damming the Nile to exploit on its resources. On the White Nile, Uganda has constructed the Bujagali dam while along the Blue Nile, Ethiopia is constructing the continent's largest dam; the Grand Ethiopian Renaissance Dam (GERD) that is expected to take several years to fill. These human-induced impacts on the Nile, coupled with those of climate variability are expected to exacerbate tension with the low stream countries fearing the cut in the Nile's total volume. Its fresh water in the region that covers approximately 10% of the entire African continent is expected to continue sustaining the livelihood of the growing population thus making a large part of the African continent extremely vulnerable in aspects such as water supplies, agriculture, and industry (Woodward et al., 2007; Awulachew et al., 2012; Multsch et al., 2017). An understanding of changes in its stored water (surface, soil moisture and groundwater), and their association to climate variability/change, is, therefore, crucial for environmental assessments and provides useful information useful for water resources management and climate impact studies. Owing to its size however, the Nile predisposes itself to remotely sensed approaches with the vast spatial and temporal coverage as opposed to ground based in-situ networks.

Remote sensing has provided useful observations for studying water resources around the world, especially over areas with insufficient in situ measurements (e.g., Alsdorf et al., 2007; Zakharova et al., 2006; Papa et al., 2010; Khaki et al., 2017a,b). Over the Nile River Basin

(NRB), Muala et al. (2014) estimated reservoir discharges of Lake Nasser and Roseires Reservoir while flood monitoring using altimetry data was carried out by Birkett et al. (1999) over Lake Victoria. Ayana et al. (2008) reviewed the application of satellite radar altimetry data in the water resource management in Ethiopia, while Uebbing et al. (2015) introduced a post-processing approach to improve the accuracy of radar altimetry measurements over African lakes such as Lake Naivasha and Lake Victoria (see also Awange et al., 2013a; Aboulela, 2012). A number of hydroclimate variability studies over the basin using various satellite remotely sensed products have been documented, e.g., the Gravity Recovery And Climate Experiment (GRACE) for studying the Nile basin's total water storage changes (e.g., Awange et al., 2008, 2014a; Hassan and Jin, 2014), satellite precipitation data for studying the basin's rainfall (e.g., Kizza et al., 2009; Awange et al., 2013b), and a combination of both ground-based and remotely sensed observations for studying the lake's water balance (e.g., Yin and Nicholson, 1998; Swenson et al., 2009).

Despite the efforts above, a comprehensive long-term study of climate variability and its association with various water storages (TWS, groundwater, surface water storage, and soil moisture) separately, as well as water level fluctuations over the entire NRB is missing. For example, Awange et al. (2014b) studied water storage changes within the Nile's main sub-basins and the related impacts of climate variability by employing Independent Component Analysis (ICA; see also Forootan and Kusche, 2012, 2013) to extract statistically independent TWS patterns over the sub-basins from GRACE and the Global Land Data Assimilation System (GLDAS) for the period 2002-2011. Their study, however, does not address variability of individual water storage compartments (surface, soil moisture and groundwater). Rather, they treated them as a combined entity and did not compute the fluctuations of the water level within the NRB. Fluctuations of surface water levels, which can be derived from satellite radar altimetry, are important as they can be related to seasonal variations of precipitation, evaporation, and anthropogenic use (Goita et al., 2012). Surface water storages and their variations are also important to study the interactions between land and the atmosphere and oceans (Papa et al., 2015).

The present study addresses these missing gaps by exploiting multi-satellites and surface models' products to study changes in the various Nile basin's water storage compartments (surface, soil moisture, and groundwater) it relates their changes to climate variability. Specifically, the study aims at (i) analyzing the long-term (1992-2016) water level fluctuations through 62 virtual altimetry-derived tide gauges along the Nile River, (ii) deriving surface water storage from level variations in (i) above, and (iii) studying compartmental water storage changes separately; surface, soil moisture, and groundwater and their association with El Niño Southern Oscillation (ENSO) and Indian Ocean Dipole (IOD) climate variability.

To provide the 62 virtual stations over the entire Nile River, TOPEX/Poseidon (T/P), Jason-1 and -2 satellite altimetry products are applied to the Nile Basin divided into Lower Nile, Central Nile, and Upper Nile (see Fig. 1). The obtained water level fluctuations from these 62 virtual stations are improved using the Extremum Retracking (ExtR) algorithm (Khaki et al., 2014, 2018a) and used to generate time series that are employed to derive surface water storage following the approach proposed by Frappart et al. (2008). Furthermore, multiple models are used to estimate soil moisture variations, while their uncertainty is estimated using the Triple Collocation Analysis (TCA; Gruber et al., 2017) within the basin. These data together with TWS changes from GRACE are applied to estimate Nile Basin's groundwater storage. The impact of climate variability (e.g., ENSO and IOD phenomena) and precipitation from the Tropical Rainfall Measuring Mission Project (TRMM) on surface water variations and water storage components are thereafter explored.

The reminder of this study is organized as follow; the study area, datasets, and methods are presented in Sect. 2 and 3, respectively. The results are discussed in Sect. 4 and the study is concluded in Sect. 5.

2. The study area and data

2.1. The Nile River Basin

Climatic conditions in the NRB vary over different parts and include different climate zones (e.g., Mediterranean climate), with an average temperature of about 30°C in summers and ranging between 5°C - 10°C during winters (FAO, 1997). The arid region starts from Sudan and extends north to Egypt with average precipitation rates of 50 mm and 20 mm per year, respectively, representing almost rainless conditions during a given year (FAO, 1997; Agrawal et al., 2003). In contrast, the southern parts of the basin from the equatorial region of south-western Sudan to most of the Lake Victoria basin and the Ethiopian Highlands experience heavy rainfall of about 1520 mm per year (Camberlin, 2009; Awange et al., 2016). A modest increase in rainfall and stored water over Lake Victoria from 2007 to 2013 after the 2002-2006 decline (Awange et al., 2008) is captured by Awange et al. (2013b) while water loss in the north-eastern lowland of Ethiopia between 2003 and 2011, in contrast to the western parts, has been observed by Awange et al. (2014a,b). Becker et al. (2010) studied the 2003-2008 water level changes in major lakes of East Africa and concluded that for Lake Victoria and Lake Turkana, changes were mainly due to individual lake's storages.

The difference between climatic conditions and water availability along the Nile has become increasingly important especially for the northern areas facing increased water scarcity, i.e., Sudan and Egypt (see, e.g., Conway, 2002; Elshamy et al., 2009; Taye et al., 2011). A number of studies have investigated the interactions between different areas along the NRB and various issues, e.g., sediments (Ahmed et al., 2008) and residents income inequality (Ahmed et al., 2014). To better study the entire basin in regard to fluctuations and the impacts of climate, the present study divides the entire NRB into three different regions; the Upper Nile, Central Nile, and Lower Nile (Fig. 1) approximated according to the provenance of the water as suggested in Ahmed et al. (2004).

2.2. Satellite radar altimetry

Satellite radar altimetry is an effective tool for monitoring surface water level fluctuations and has been employed for a wide range of applications (e.g., Sandwell, 1990; Fu et al., 1994; Lee et al., 2009; Hwang et al., 2010; Becker et al., 2010; Khaki et al., 2015). Application of altimetry for monitoring inland water lakes (see, e.g., Birkett, 1995) and rivers (e.g., Birkett et al., 2002; Berry et al., 2005; Yang et al., 2012; Tseng et al., 2013) is growing because of its vast coverage contrary to ground-based measurements (Calmant et al., 2008). In this study, we use TOPEX/Poseidon (T/P), Jason-1, and Jason-2 data of the Sensor Geographic Data Records (SGDR), which contains 20-Hz waveform data. This includes 360 cycles of T/P covering 1992–2002, 260 cycles of Jason-1 from 2002 to 2008, and 277 cycles of Jason-2 covering 2008 to 2016. The temporal resolution of these observations is ∼9.915 days and their ground cross-track resolution is ∼280 km (Benada, 1997). T/P and Jason-1 data are both derived from the Physical Oceanography Distributed Active Archive Center (PO.DAAC) and Jason-2 data is provided by AVISO (see, e.g., Table 1). Here, we apply geophysical corrections, including solid earth tide, pole tide, and dry tropospheric (Birkett, 1995). Importantly, the waveform

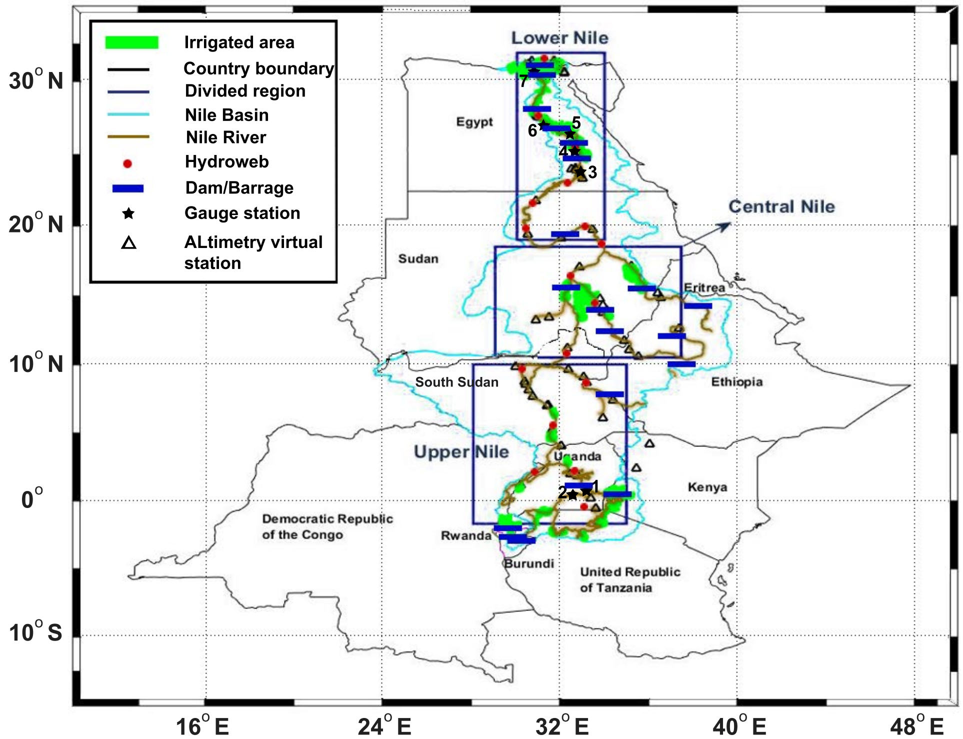

Figure 1: Location of the 62 virtual altimetry stations and the three study regions; Upper Nile (Kenya, Uganda, Tanzania, Rwanda, Burundi, Ethiopia and South Sudan), Central Nile (Sudan, Ethiopia and Eritirea), and Lower Nile (Egypt) in the Nile Basin. This figure also contains the positions of the gauge stations and Hydroweb (Cretaux et al., 2011) for measuring water levels, as well as major infrastructures (e.g., dams) and irrigation areas (following The Food and Agriculture Organization (FAO) and Multsch et al., 2017).

retracking, which refers to the re-analysis of the waveforms, a time-series of returned power in the satellite antenna (Davis et al., 1995; Gomez-Enri et al., 2009), is required to improve the accuracy of measured ranges (Brown, 1977). Here, in order to retrack satellite radar altimetry data, a developed Extrema Retracking (ExtR) algorithm proposed by Khaki et al. (2014) is applied. Our motivation to select the ExtR is due to its processing speed and its promising results while various types of waveforms are observed (see, e.g., Khaki et al., 2015, 2018b). ExtR has already been compared to the Off Center of Gravity (OCOG, Wingham et al., 1986), the NASA β-Parameter Retracking (Martin et al., 1983), and Threshold Retracking (Davis, 1997) techniques.

The datasets are then used to build virtual time series for 62 different points (see black triangles in Fig. 1) located on the satellite ground tracks and distributed throughout the NRB. At each virtual point, several points belonging to the same satellite cycle are considered and the median value of the retracked altimetry-based water level is computed in order to address the hooking effects (Frappart et al., 2006). This effect is derived from off-nadir measurements when a satellite locks over a water body before or after passing above it (Seyler et al., 2008; Boergens et al., 2016). Afterward, the water level variations time series derived from T/P, Jason-1, and Jason-2 (covering the period from 1992 to 2016) are merged and the combined time series converted into a monthly scale. Note that the maximum number of stations available from satellite radar altimetry over the area is used to better represent the water level variations over the NRB. Nevertheless, when comparing with other datasets (e.g., precipitation), provided at $1°\times1°$ spatial resolution, altimetry-derived data from stations located in a grid point (i.e., $1°\times1°$) are averaged. The average of water level data in the grid point is then compared with other data from the same point. Details of altimetry data sources and pass numbers used in this study are presented in Table 1.

2.3. GRACE

Monthly GRACE level 2 (L2) potential coefficients products up to degree and order (d/o) 90 from the ITSG-Grace2014 gravity field model (Mayer-Gürr et al., 2014) are obtained and used to generate total water storage (TWS) within the NRB. Following Swenson et al. (2008), degree 1 coefficients (http://grace.jpl.nasa.gov/data/get-data/geocenter/) are replaced to account for the movement of the Earth's centre of mass. Degree 2 and order 0 (C_{20}) coefficients (http://grace.jpl.nasa.gov/data/get-data/oblateness/) are not well determined, and therefore, they are replaced by those from Cheng and Tapley (2004). Colored/correlated noise and leakage errors are reduced using the Kernel Fourier Integration (KeFIn) filter (Khaki et al., 2018c) in a two-step post-processing scheme. The first step accounts for the measurement noise and the aliasing of unmodelled high-frequency mass variations, and the second step reduces the leakage errors (see also Khaki et al., 2018d).

2.4. Land hydrological models

Soil moisture data is provided from three sources; the Famine Early Warning Systems Network (FEWS NET) Land Data Assimilation System, (FLDAS-NOAH; McNally et al., 2017), the WaterGAP Global Hydrology Model (WGHM; see more details in Döll et al., 2003), and ERA-Interim (Dee et al., 2011). Soil moisture outputs from these models are acquired on a monthly scale and rescaled into $1°\times1°$ spatial grid and merged into a single soil moisture product (using TCA, see Sect. 3.2.2) to study the soil moisture variations within the NRB, as well as extracting groundwater from GRACE's TWS and surface water storage estimates (see Sect. 3.2).

2.5. Precipitation

The Tropical Rainfall Measuring Mission (TRMM-3B43; version 7) products (TRMM, 2011) covering the period 1998 to 2016 are used to estimate how much water enters the NRB. The data is available on a 0.25° degree resolution, which is averaged to generate $1°\times1°$ grids before being extended to 1992 (same starting period as the altimetry data) using the Global Precipitation Climatology Center (GPCC) reanalysis version 7.0 (Schneider et al., 2015).

2.5.1. ENSO and IOD

Two major climate variability indices associated with the dominant SST variability; El Niño Southern Oscillation (ENSO; Barnston et al., 1987) and Indian Ocean Dipole (IOD; Rao et al., 2002) are used to assess the association of climate variability and NRB's stored water changes. ENSO, provided by the NOAA National Centers for Environmental Information (NCEI) between 1992 and 2016, is the largest inter-annual climate variability phenomenon in the Tropical Pacific, which affects the climate of many regions of the Earth (Trenberth et al., 1990; Forootan et al., 2016). El Niño refers to the positive phase of ENSO that brings warm water towards the east of the Americas causing a climate shift over the Pacific. The opposite phase La Niña causes less than normal precipitation variability (Nazemosadat et al., 2000) in the western Pacific, and to the north of Australia. An ocean-atmosphere phenomenon measure that indicates changes in sea surface temperature in the Indian Ocean is IOD (Indian Ocean Dipole). Its data is acquired from NASA's Global Change Master Directory (GCMD). A positive IOD (often associated with El Niño) causes cooler waters (and droughts) near Australia and Southeast Asia and brings warmer than normal water and heavy rains in East Africa and India. A negative IOD, on the other hand, brings the opposite conditions, e.g., larger precipitation in the eastern Indian Ocean, and cooler conditions in the west. These indices are the result of interactions between the oceans and atmosphere on each corresponding area and their impact can be seen directly on rainfall that occurs around the world (Nurutami et al., 2016). Here, the interest is to understand their influences on the Nile River fluctuations, thereby, further indicating the impact of climate variability. A summary of the datasets used in the present study are presented in Table 1.

Table 1: A summary of the datasets used in this study.

		Data resolution			
Description	**Source**	Spatial	Temporal	**Detail**	**Data access**
Altimetry-derived level height	T/P, Jason-1	~280 km	~9.915	Pass numbers 18, 31, 44, 57, 83, 94, 107, 120, 133, 159, 170, 196, 209, 222, 235	http://podaac.jpl.nasa.gov
	Jason-2	~280 km	~9.915	Pass numbers similar to T/P, Jason-1	http://avisoftp.cnes.fr/
Precipitation	GPCC	1°	Monthly	Global precipitation climatology center (GPCC) reanalysis version 7.0	https://www.esrl.noaa.gov/psd/data/gridded/data.gpcc.html#detail
	TRMM-3B43	0.25°	Monthly	Tropical Rainfall Measuring Mission Project (TRMM) version 7.0	https://disc.gsfc.nasa.gov/datacollection/TRMM_3B43_7.html
Terrestrial water storage (TWS)	GRACE	~300 km	Monthly		https://www.tugraz.at/institute/ifg/downloads/gravity-field-models/itsg-grace2014/
Soil moisture	WGHM	0.5°	Monthly		https://www.uni-frankfurt.de/45218093/Global_Water_Modeling
Soil moisture	ERA-Interim	0.5°	Monthly		https://www.ecmwf.int/en/forecasts/datasets/reanalysis-datasets/era-interim
Soil moisture	FLDAS	0.5°	Monthly	Famine Early Warning Systems Network (FEWS NET) Land Data Assimilation System (first soil moisture layer)	https://disc.sci.gsfc.nasa.gov/uui/datasets/FLDAS_VIC025_C_SA_M_V001/summary?keywords=FLDAS
ENSO		~280 km	Monthly		https://www.ncdc.noaa.gov/teleconnections/enso/
IOD		~280 km	Monthly		http://gcmd.nasa.gov/records/GCMD_Indian_Ocean_Dipole.html
Water level measurements		–	–	Ministry of Energy & Mineral Development Kampala, Uganda	http://www.energyandminerals.go.ug/

3. Method

3.1. Extrema Retracking (ExtR) and the validation of its output

In order to retrack satellite radar altimetry data over the NRB, the Extrema Retracking (ExtR) post-processing technique of Khaki et al. (2014) is employed. It is applied to the altimetry-derived waveforms to retrack datasets, what is vital for inland applications of satellite radar altimetry. The algorithm operates in three steps (1) a moving average filter is applied to reduce the random noise of the waveforms, (2) extremum points of the filtered waveforms are identified, and (3) the leading edges among all detected extremum points are explored. Range corrections are applied using the offsets between the positions of the leading edges and their on-board values. To assess the performance of the ExtR filter, its results are evaluated against those of in-situ (see Fig. 1) height variations. To this end, use is made of (i) monthly water level measurements from two gauge stations (Jinja 1992-1995 and Entebbe 1992-2009) obtained from the Ministry of Energy & Mineral Development (Kampala, Uganda), (ii) in-situ data obtained from Ismail and Samuel (2011). These are; old Aswan 1996-2009, Esna Barrage 1996-2009, Naga Hammadi Barrage 1996-2007, and Assiut Barrage 1996-2009, and (iii), Nubaria (1997-2007) in-situ data obtained from Samuel (2014). The Root-Mean-Squared Errors (RMSE) and the correlation coefficient between the variations of altimetry-derived height time series (with and without the application of the ExtR) at the closest virtual stations to the gauge locations and in-situ time series measurements are presented in Table 2.

The Results indicate that applying retracking method increases the correlation coefficients between altimetry results and the gauge levels (0.33 on average) and improves the RMSE by 37.56% (on average). Due to a limited number of validating gauge stations in the area, water level time series from the Hydroweb project by LEGOS (Laboratoire d'Etude en Geophysique et Oceanographie Spatiale; Cretaux et al., 2011) and DAHITI (Database for Hydrological Time Series of Inland Waters; Schwatke et al., 2015) were further used. Fig. 2 shows a sample time series over Lake Victoria within the Upper Nile derived from the ExtR filter compared to the Hydroweb and DAHITI time series. It can be seen from the figure that the ExtR time series are close to the retracked time series of DAHITI (i.e., 0.94 average correlation coefficient) and to a lesser degree to Hydroweb (i.e., 0.92 on average). Overall, the correlation coefficients from both Hydroweb and DAHITI are high (i.e., > 0.90) and are statistically significant at 95% confidence level thus indicating a good performance of ExtR. More virtual stations are provided by Hydroweb along the Nile River (see Fig. 1), which are used for comparison with the ExtR results. The average estimated RMSE and correlation coefficients are presented in Table 2. The ExtR results are 37.44% (on average at 95% confidence level) more correlated to Hydroweb data. Based on these in-situ validations, the ExtR algorithm is further justified and thus employed in this study to retrack satellite radar altimetry data.

3.2. Water storage changes

Assuming the contribution of ice/snow and vegetation to be negligible over the NRB, changes in TWS (ΔTWS) can be sufficiently taken to be the summation of changes in surface water (ΔSr), soil moisture (ΔSm), and groundwater (ΔGr) storages (see, e.g., Khaki et al., 2017c, 2018d) as,

$$\Delta TWS = \Delta Sr + \Delta Sm + \Delta Gr. \tag{1}$$

Table 2: A comparison between satellite altimetry values derived from the ExtR retracking method and those from in-situ water level measurements. The improvements in the RMSE are calculated using the in-situ measurements in comparison to the raw altimetry data.

	Raw altimetry data		ExtR retracking		
Stations	**RMSE** (cm)	**Correlation coefficient**	**RMSE** (cm)	**Correlation coefficient**	**Improvement (%)**
(1) Jinja	48.49	0.52	31.45	0.78	35.14
(2) Entebbe	61.14	0.66	36.04	0.95	41.05
(3) Old Aswan	36.77	0.54	22.44	0.88	38.97
(4) Esna	27.27	0.52	15.36	0.91	43.67
(5) Naga Hammadi	38.73	0.61	28.12	0.82	27.40
(6) Assiut	42.62	0.57	25.89	0.93	39.26
(7) Nubaria	25.87	0.62	16.19	0.92	37.44
(8) Hydroweb	56.13	0.59	29.28	0.94	47.83

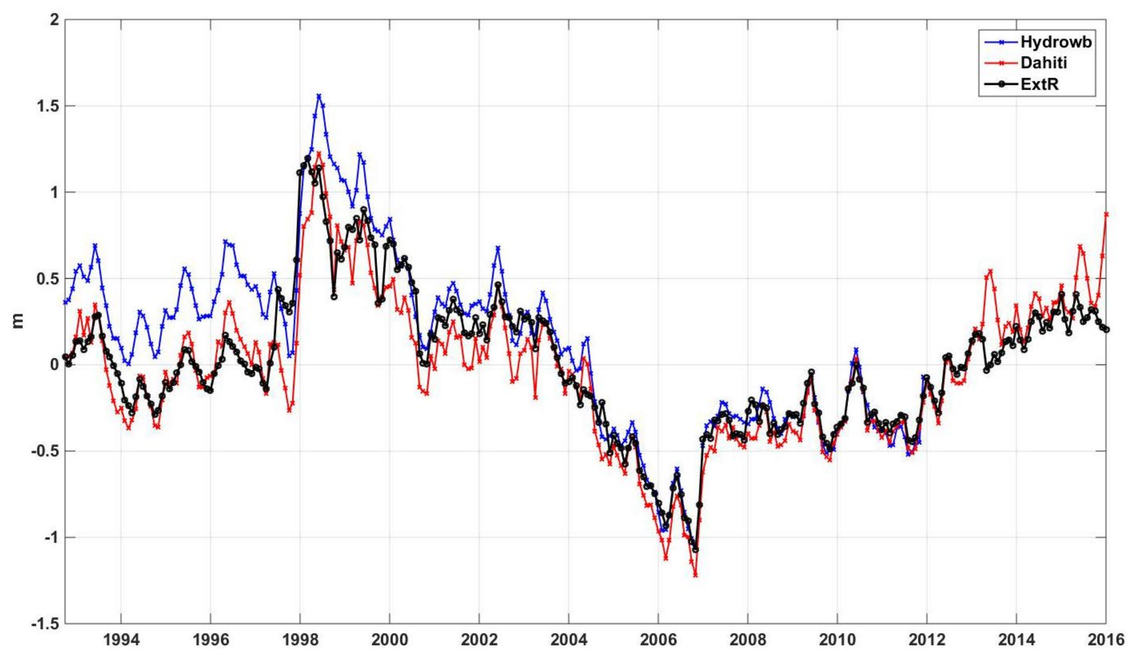

Figure 2: A comparison between monthly height time series (after removing the long-term mean) of Lake Victoria obtained from the ExtR retracking method (black), DAHITI (red), and HYDROWEB (blue). The results of ExtR retracking method are highly correlated with those of HYDROWEB and DAHITI (i.e., > 0.90; significant at 95% confidence level). This justifies the usage of the ExtR retracking method to obtain the surface heights of the 62 virtual stations along the NRB.

GRACE products provide the total water storage changes ΔTWS while ΔSr are calculated from water level measurements as discussed in Sect. 3.2.1. The changes in soil moisture ΔSm are estimated from multi-models' outputs as discussed in Sect. 3.2.2. Using these estimates of ΔSr and ΔSm in Eq.1, the estimates of groundwater ΔGr within the NRB are derived.

3.2.1. Surface water storage changes

To calculate changes in surface water storage from water level data, the approach proposed in Frappart et al. (2008) is used. The process begins by generating water level maps at monthly scales using altimetry-derived in-situ and Hydroweb time series across the NRB. These maps are constructed at $1^{\circ}\times1^{\circ}$ (similar to those of GRACE TWS) using point-wise water level time series and a bilinear interpolation scheme to estimate water levels at each grid point. Afterwards, the surface water volume changes (ΔSr) between two consecutive months i and $i-1$ within the basin S, corresponding to the difference of surface water level maps, is estimated by (see, e.g., Frappart et al., 2008, 2011),

$$\Delta Sr(i,i-1) = R_e^2 \delta\lambda\delta\theta \sum_{j \in S} P_j \delta h_j(\lambda,\theta,i,i-1) sin(\theta_j), \tag{2}$$

where $\delta\lambda$ and $\delta\theta$ are the sampling grid steps in longitude (λ) and latitude (θ) directions, respectively. R_e is the mean radius of the Earth ($\sim 6378\,km$), δh represents the difference of surface water levels, and $R_e^2 sin(\theta_j)\delta\lambda\delta\theta$ corresponds to the surface of grid element j. The percentage of inundation P_j is acquired from Multisatellite Inundation Data Set approach (Prigent et al., 2001, 2007).

3.2.2. Soil moisture changes

In order to achieve more reliable estimates of soil moisture changes over the NRB, data from three different sources (FLDAS-NOAH, WGHM, and ERA-Interim) are merged using the Triple Collocation Analysis (TCA; Awange et al., 2016; Gruber et al., 2017) following Stoffelen (1998). TCA is chosen since in the absence of ground reference data, it offers an alternative method for estimating random error variances (Gruber et al., 2017). TCA is applied here to merge soil moisture outputs;

$$S_1 = \alpha_1 S_t + e_1, \tag{3}$$

$$S_2 = \alpha_2 S_t + e_2, \tag{4}$$

$$S_3 = \alpha_3 S_t + e_3, \tag{5}$$

with S_t being the true soil moisture variation, S_1, S_2, and S_3 represents three soil moisture anomalies related to S_t with α_1, α_2, and α_3 being the coefficients that correspond to the errors of e_1, e_2, and e_3, respectively. The objective is to estimate error variances associated with e_1, e_2, and e_3 to be used in the weighting process. On the one hand, TCA solves this by considering the errors of the products to be independent of each other while on the other hand, it arbitrarily assumes any of the products as a reference (see Stoffelen, 1998; Yilmaz et al., 2012, for more details regarding TCA implementation). By selecting any of the products as the reference, no impact is imposed on the merged time series (Gruber et al., 2017). Once the error variances are calculated, they are used in Eq. 6–8 to estimate weights of each merged product through

$$w_1 = \frac{\sigma {S_2}^2 \sigma {S_3}^2}{\sigma {S_1}^2 \sigma {S_2}^2 + \sigma {S_1}^2 \sigma {S_3}^2 + \sigma {S_2}^2 \sigma {S_3}^2}, \tag{6}$$

$$w_2 = \frac{\sigma {S_1}^2 \sigma {S_3}^2}{\sigma {S_1}^2 \sigma {S_2}^2 + \sigma {S_1}^2 \sigma {S_3}^2 + \sigma {S_2}^2 \sigma {S_3}^2}, \tag{7}$$

$$w_3 = \frac{\sigma {S_1}^2 \sigma {S_2}^2}{\sigma {S_1}^2 \sigma {S_2}^2 + \sigma {S_1}^2 \sigma {S_3}^2 + \sigma {S_2}^2 \sigma {S_3}^2}, \tag{8}$$

where $\sigma {S_1}^2$, $\sigma {S_2}^2$, and $\sigma {S_3}^2$ are error variances of S_1, S_2, and S_3, respectively, with the corresponding weights of w_1, w_2, and w_3. The final merged soil moisture estimate (Sm) is obtained by,

$$Sm = w_1 S_1 + w_2 S_2 + w_3 S_3. \tag{9}$$

A schematic illustration of the applied processing steps in this study, i.e., data integration procedure, retracking, and water storage estimations, is provided in Fig. 3.

4. Results and discussion

4.1. River height variations

First, a review of the altimetry-derived river level height time series (Fig. 4) is undertaken to understand the river's fluctuations with time. Thus, water lever time series is calculated for each virtual station within the three study regions of Fig. 1. The average of the stations' level height variations after removing the long-term mean in each region is presented in Fig. 4. Also, the trend for different parts of time series are plotted (cf. black solid lines in Fig. 4). As can be seen from Fig. 4, despite some similar behaviours such as positive trends after 2007 for all regions, the river height fluctuations differ from region to region. Between 1992-2002, water levels rose in the Upper and Central Nile regions, while in contrast, over the same period of time, water level fell at a rate of 0.01 m/year in the Lower Nile region. Moreover,

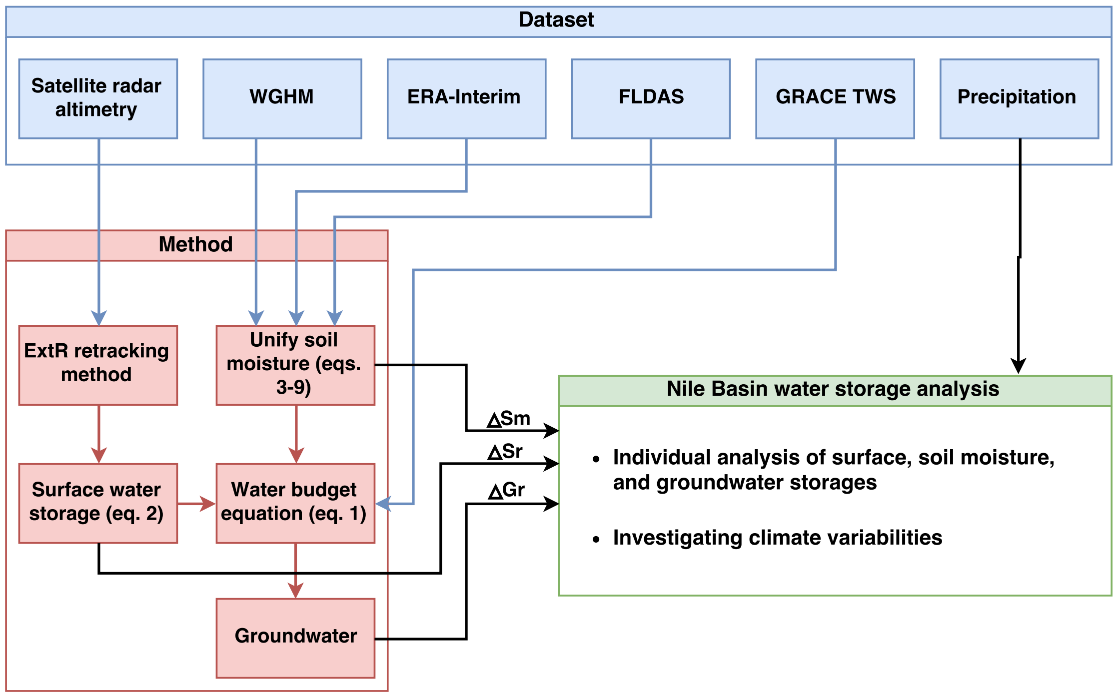

Figure 3: A schematic illustration of the applied methodology. The figure shows how the various stored water compartments; surface water, soil moisture and groundwater of the NRB are generated from multi-satellite and multi-models.

unlike the Upper and Central Nile regions, the Lower Nile region experienced water level fall in 2002. The Upper Nile region shows remarkably larger variations possibly due to higher rainfall in the region.

A decrease in the Upper Nile's water levels between 2002 and 2006 is consistent with the findings of Awange et al. (2008) and Swenson et al. (2009), where excessive dam construction (e.g., expansion of the Nalubaale Dam to include Kiira Dam) contributed to the fall. A similar negative trend is observed in the Lower Nile (0.76 average correlation coefficient between water levels of the Upper and Lower Nile) and Central Nile (0.68 on average). These correlation coefficients depicts the effects of Upper Nile's water management policies (e.g., dam constructions) on the other regions. The small change in the Central Nile during the period 2002-2006 compared to the Upper Nile could indicate other factors (e.g., climatical) since the Blue Nile comes from the Ethiopian highlands and as such was not impacted by the expansion of the dam in Uganda. This can explain the lower correlation coefficient between water level variations in Upper Nile and the Central Nile in comparison to the Lower Nile. The rate of fall in 2002-2006 in the lower

Nile is higher than the upper and Central Nile as a result of the possible combined effects of anthropogenic (Upper Nile; for example irrigation, see, e.g., Sultan et al., 2013; Awange et al., 2014b) and climatic (Central Nile) origins.

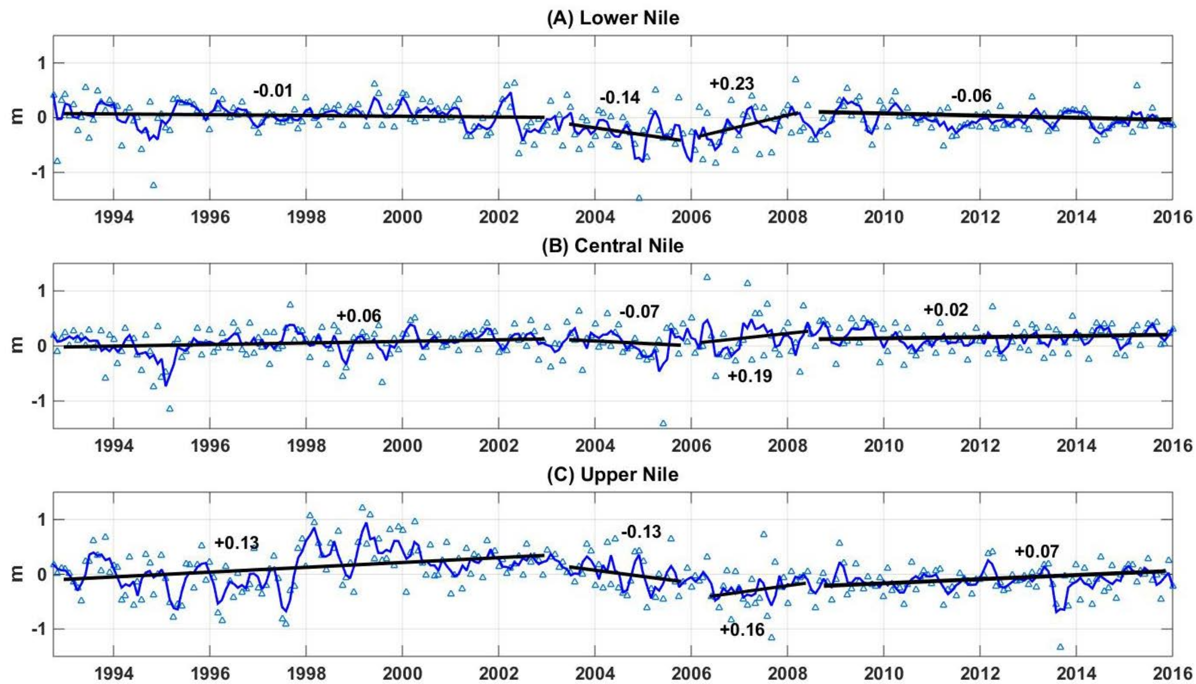

Figure 4: Monthly river level height variations (blue triangles) and their 60-day smoothed (for a better presentation) time series (blue lines) for each region. Variation rate (m/year) are reported above the fitted lines (black lines). Note that long-term average height levels are removed from each time series.

After 2006, water levels rose in all the three regions until 2008 at different rates (i.e., 0.16 m/year for Upper Nile region, 0.19 m/year for Central Nile and 0.23 m/year for the Lower Nile region). The main reasons for this are positive precipitation rates (cf. Fig. 5), and the fact that the excessive exploitation of the White Nile for hydroelectric purposes by Uganda reduced (see, e.g., Awange et al., 2008; Swenson et al., 2009). The differences between water level rise rates over the three regions could be attributed to climatic impacts. For example, the ENSO rainfall of 2007 (Omondi et al., 2013) brought heavy rainfall to the East African region and caused water level increase in the Nile region. In addition, La Niña impacts, which caused drought in Ethiopia led to a smaller water level increase in the Central Nile compared to the Lower Nile, where the Blue Nile contribution resulted in a larger increase. Same positive trends can also be seen after 2008 over Upper and Central Niles. The positive trend is smaller over Central Nile possibly due to the fact that the White Nile's waters are lost in the Sudd-wetland (Awange et al., 2014a), hence, the diminishing effect of the increase can be seen from the Upper Nile to the Central Nile. Lower Nile, on the other hand, depicts a negative water level variation rate for the same period. The Lower Nile reflects already reduced water level variation rate of the Central Nile plus withdrawal effects for irrigation purposes (cf. Fig. 1 for irrigated areas, see also Sultan et al., 2013; Awange et al., 2014b). This could also explain larger negative trends between 2002 and 2006, where water use aggravates the excessive dam construction in Upper and Central Niles (see, e.g., Fig. 1). Moreover, as it will be shown in Fig. 5, negative precipitation rates for the periods of 1992–2002 and 2002–2006 result in surface water decline over the same periods in Lower Nile.

4.2. Water storages: surface, soil moisture and groundwater

Following Frappart et al. (2008), surface water storage is derived from water level fluctuations over the NRB. The average surface storage time series for the Upper, Central, and Lower Nile regions are shown in Fig. 5. The average time series of precipitation and GRACE TWS are also shown in the figure. It can be seen from the figure that the time series generally follow water level variation patterns of Fig. 4. The Upper Nile's time series depicts larger variations with various trends (see also the Lower Nile with a negative trend) unlike the Central Nile. Similar to the water level variation time series in Fig. 4, various smaller (short-term) trends can be seen, particularly for the Upper and Lower Nile regions. The negative trend in surface water seen before 2002 in the Lower Nile does not exist in the Upper or Central Nile regions possibly due to extensive usage in activities such as irrigations (see, e.g., Sultan et al., 2013).

Overall, the largest fluctuations are observed in the Upper Nile mainly due to high precipitation. TWS changes naturally follow the precipitation and hence a similar pattern can also be seen. This is followed by the Central Nile, which shows larger variations in both precipitation and TWS time series compared to the Lower Nile (a region with the least precipitation). As with water level variations (cf. Fig. 4), negative surface water storage trends exist in all the three regions (see Fig. 5) between 2002 and 2006 due to similar reasons discussed in Sect. 4.1. This, however, is followed by positive trends in all the regions thanks to the two strong rainfall anomalies in 2006–2007 and 2010–2011 (Awange et al., 2014b). These trends are also evident in TWS variations over the Central and Upper Nile. Nevertheless, it can be seen that the TWS variation over the Lower Nile is generally negative, which can be attributed to larger water usages in the region as discussed in Sect. 4.1. Low precipitation during this period can also be responsible for some parts of this TWS negative changes.

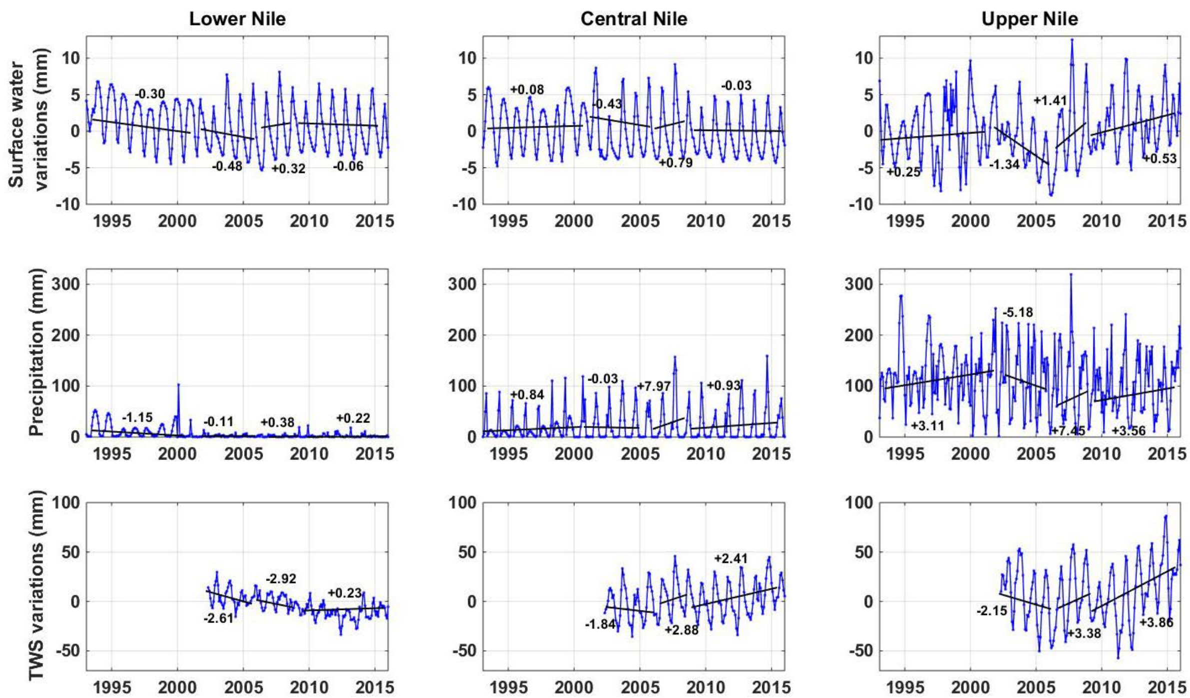

Figure 5: Average monthly surface water storage, precipitation, and TWS variations (after removing the long-term mean) over the Lower, Central, and Upper Nile regions. Variation rate (mm/year) are reported above the fitted lines (black lines). The temporal coverage of TWS is limited to 2002 to 2016 subject to the availability of GRACE data.

The impacts of precipitation on TWS variations and also surface storage changes can be seen in Fig. 5. This is evident from strong rise and fall in both surface water storage and TWS variations' time series followed by rainfall pattern. For example, 1997–1998 El Niño event (Lyon and Mason, 2007) contributed to more seasonal rainfall over Upper Nile, and correspondingly surface storage increase as indicated in Fig. 5. This, along with positive IOD event, led to highly unstable air and catastrophic floods over Equatorial East Africa (Goddard and Graham, 1999), which also caused water level increase of Equatorial Lakes (see also Birkett et al., 1999; Mistry and Conway, 2003). Strong precipitation in 2000 largely affected surface storage, especially over Upper and Central Niles. McSweeney et al. (2010) revealed the annual precipitation increases during the 1990s and 2000s, as well as a drought period of 2002–2003. The impact of this drought can clearly be seen in TWS and surface water variations (cf. Fig. 5). The 2007 ENSO rainfall (Omondi et al., 2013) has the same impact on both surface water and TWS time series. The 2011 drought over the basin (AMCEN et al., 2011; Awange et al., 2014b) is found to remarkably impacts on TWS and surface water storage. Drought conditions in Central and Lower Niles during 2015 can be attributed to an intense El Niño year (suggested by Massachusetts Institute of Technology, 2017).

The results of TCA are presented in Fig. 6, which shows the average estimated soil moisture variation from FLDAS-NOAH, WGHM, and ERA-Interim over the Lower, Upper, and Central Nile regions. Furthermore, using the surface water storage, soil moisture, and TWS changes, groundwater changes calculated based on Eq. 1 are also presented in Fig. 6. Following the patterns of precipitation and TWS time series in Fig. 5, smaller soil moisture and groundwater variations exist over the Lower Nile and to a lesser degree over the Central Nile compared to the Upper Nile while no considerable trend is observed in soil moisture variations. It is worth mentioning that seasonal variabilities for Lower Nile time series have considerably lower magnitudes in comparison to other regions. This small variability, which has also recently been shown by Ahmed and Abdelmohsen (2018) and Bonsor et al. (2018) can largely be explained by lower precipitation rate (cf. Fig. 5) over Lower Nile. Groundwater changes exhibit short-term and long-term trends over different regions. Negative trends can be seen between 2002 and 2006 generally over the Upper and Central Nile, followed by remarkable increases, likely due to the same reasons explained earlier (see also Awange et al., 2008). More importantly, a negative groundwater trend is dominant over the Lower Nile. This trend exists over the entire study period regardless of precipitation trends, which shows considerable groundwater depletion over the region. The rate of this decline, however, is found to be larger after 2008. As explained, reducing water controls in the Upper Nile after 2006 and the impact of the 2007 ENSO likely caused groundwater increase over the Central and Upper Nile and smaller negative trend over the Lower Nile. Nevertheless, this effect is found to be degraded by 2008 resulting in negative trends (with a higher rate for the Lower Nile) in all groundwater time series between 2008 and 2012. Increasing amount of precipitation after 2012 caused groundwater to rise in both Upper and Central Niles. This high rainfall has the same impact on soil moisture variation between 2012 and 2016.

For each water storage compartment (surface water storage, groundwater, and soil moisture variations), the time series are averaged over each grid point for the period of 2002 to 2016 to generate the spatial pattern maps displayed in Fig. 7. It can clearly be seen that the Lower

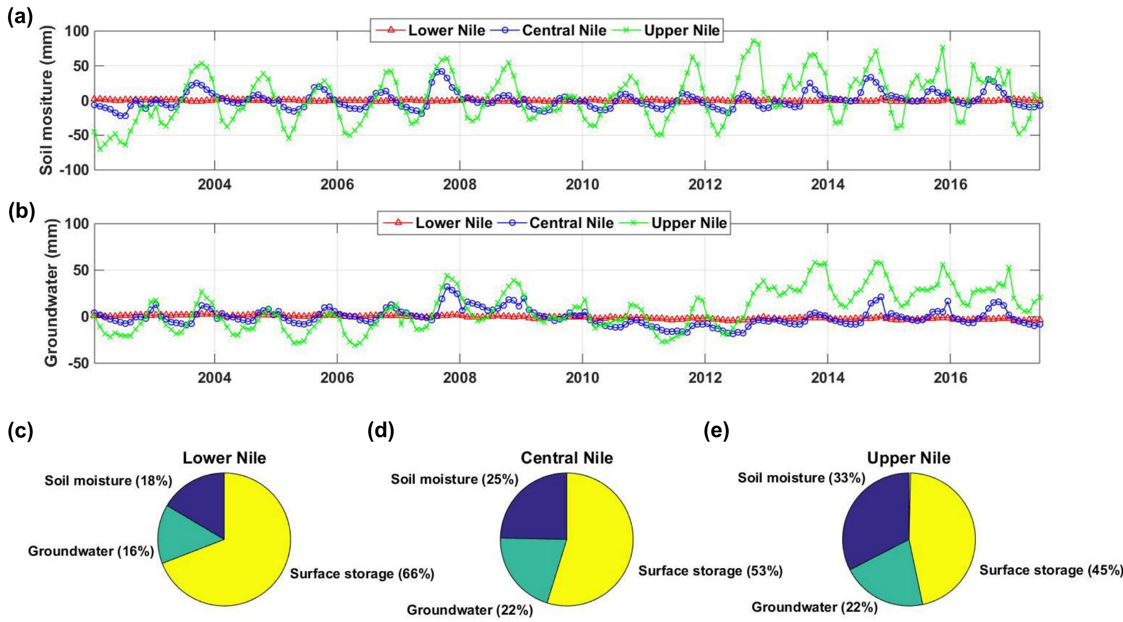

Figure 6: Average monthly soil moisture (a) and groundwater (b) variations (after removing the long-term mean) over the Lower, Central, and Upper Nile. The contributions of each water compartment in TWS (cf. Eq.1) are presented in (c) Lower Nile, (d) Central Nile, and (e) Upper Nile.

Nile depicts negative variations in the surface storage and groundwater. The Central Nile on the other hand does not show considerable change in most of the cases. Larger variations in terms of amplitude are found in the Upper Nile, thus confirming the previous findings. Besides negative groundwater changes in Egypt indicating huge usage (cf. Sultan et al., 2013; Awange et al., 2014b), Sudan and South Sudan also show considerable decline. In terms of surface water storage, the Upper Nile generally depicts positive variations.

To better compare the water storage changes within the various compartments, Fig. 8 show surface storage and groundwater trends neglecting those of soil moisture that indicated no considerable change in Fig. 6. Negative trends are observed for both surface water and groundwater storages over the Lower Nile, with the latter being more prominent thus corroborating the conclusions of Sultan et al. (2013) and Awange et al. (2014b). No considerable surface storage trend is found for the Central Nile while the Upper Nile depicts positive values. Negative trends can also be seen in some parts of the Central Nile (e.g., in some parts of Sudan and Ethiopia) and in the Lower Nile (mostly in Egypt). In contrast, most parts of the Upper Nile shows positive groundwater trends.

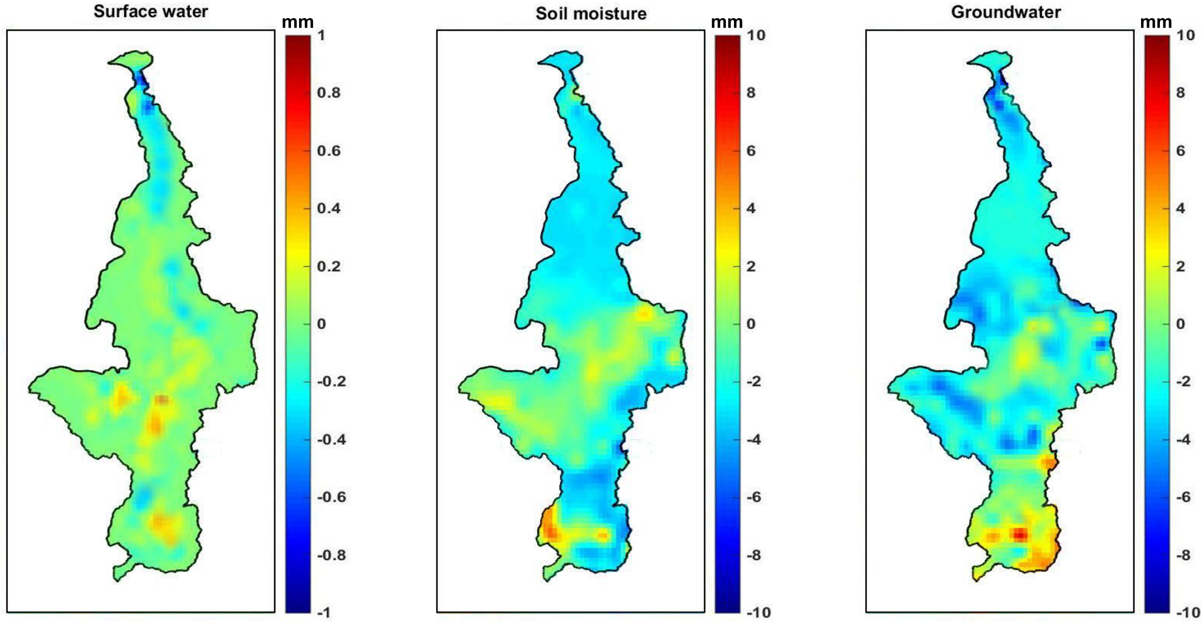

Figure 7: Temporally averaged surface water storage, soil moisture, and groundwater over the Nile Basin for the period 2002-2016.

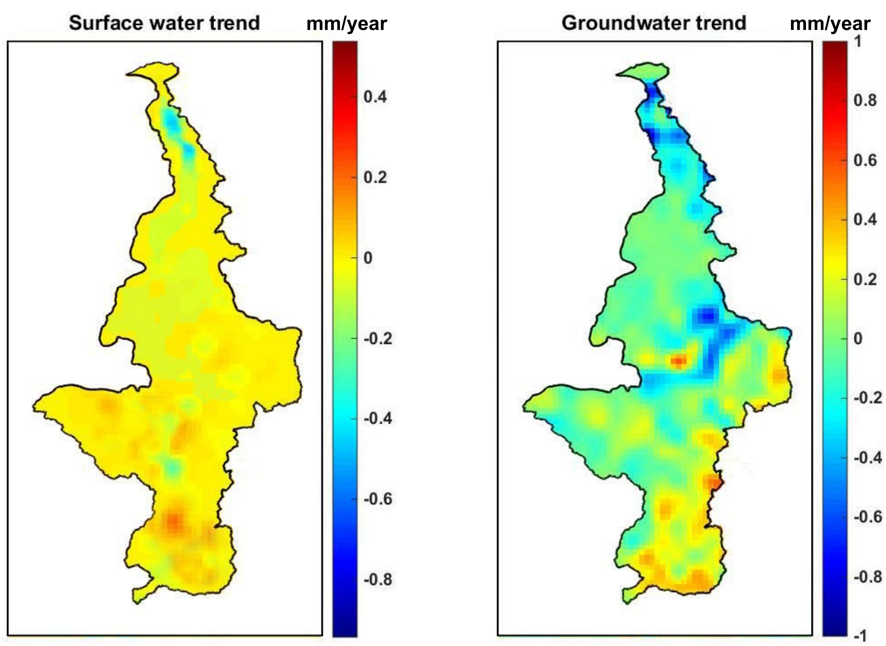

Figure 8: Surface water storage and groundwater trend over the Nile Basin for the period of 2002 to 2016. Trends of soil moisture that indicated no considerable change in Fig. 6 are neglected here.

Table 3: Correlation coefficients (at 0.05 significant level) between the river level heights, precipitation, and TWS time series for each region and climate variabilities of ENSO and IOD. Note that cross-correlation is applied to account for lag differences between the time series.

Climate index	Variable	Lower Nile	Central Nile	Upper Nile
ENSO	Water level	0.47	0.52	0.58
	Precipitation	0.61	0.68	0.72
	TWS	0.58	0.64	0.69
IOD	Water Level	0.41	0.44	0.45
	Precipitation	0.52	0.54	0.59
	TWS	0.43	0.48	0.55

4.3. Global teleconnections

In order to further understand the interactions of precipitation, river level heights, and TWS with climate variabilities, their correlation coefficients with ENSO and IOD climate variability indices are calculated for each region and presented in Table 3. Those of IOD are found to be generally lower than ENSO's. Table 3 show the highest correlation coefficient to be between ENSO and precipitation especially for the Upper Nile. For the correlations between ENSO and TWS, the highest value is also achieved in the Upper Nile probably due to the strong connection between precipitation and TWS over the region (see e.g., Awange et al., 2014a). For all variables (water level, precipitation, and TWS), the smallest correlation coefficients are achieved in the Lower Nile, a factor which can be attributed to very limited precipitation on the one hand, and high human impacts on water storages on the other hand (e.g., Sultan et al., 2013). Comparing ENSO's correlation coefficients between water levels and TWS, larger values are obtained with TWS. This can be explained by the fact that contrary to the water level fluctuations, non-climatic impacts on TWS are smaller. Considering the entire NRB, a higher correlation coefficient between the river level heights and climate indexes are found in the Central Nile (0.52 for ENSO). The addition of the Blue Nile in this area could possibly explain this higher correlation coefficient in comparison to the other regions.

5. Conclusion

This study analyzed the Nile River water level fluctuations and total water storage (TWS) compartments (surface water, soil moisture, and groundwater storage) using multi-mission satellite products, as well as land surface models. The association between these variables and climate variabilities are also investigated using precipitation and ENSO time series.

This is crucial for water management policies of the Nile Basin Authority that manages the water resources on behalf of the eleven countries whose livelihood is highly dependent on the Nile for various aspects, e.g., water supply, agriculture, and industry. Importantly, we showed that water usages over the Upper Nile can largely impact the Nile's water variations in Central Nile and particularly Lower Nile, as seen e.g., between 2002–2006 (Awange et al., 2008). Excessive dam and barrage constructions, e.g., by Uganda, Rwanda, Kenya, and Ethiopia should be controlled due to their immediate influence on water availability on other parts, e.g., Egypt, which relies on the Nile. It was also found that climatic impacts can also be very important over the entire basin, such as frequent droughts over Central and Lower Nile, and flood events over the Upper Nile. The following summarizes the major outcomes of the study.

- A considerable long-term (2002-2016) negative groundwater trend is found in the Lower Nile (Egypt) signifying a potential depletion. The rate of decline is seen to increase rapidly from 2008 despite increase in precipitation and TWS time series, thus signifying the possibility of human usage, e.g., for irrigation purposes. Smaller soil moisture and groundwater variations exist over the Lower Nile and to a lesser degree over the Central Nile compared to the Upper Nile. While no considerable trend is observed for soil moisture variations, groundwater changes exhibit short-term and long-term trends over different regions. Negative trends are found between 2002 and 2006 over the Upper and Central Nile.

- The Upper Nile, the headwaters of the White Nile, depicts large water level variations compared to the Central (region covering the Blue Nile) and the Lower Nile (Egypt and Sudan). In general, a negative trend is found for water level variation in the Lower Nile (with the highest for the period 2002 – 2006) in contrast to the Central and Upper Nile.

- Stronger correlation between the river level variations and precipitation exist in the Central Nile compared to the Upper and Lower Nile regions over the study period. The contribution of the Blue Nile (originating from the Ethiopian highlands) appears to cushion the Central Nile.

- Larger precipitation and TWS variations exist in the Upper Nile and to a lesser degree over the Central Nile, which can explain larger water storage fluctuation in these regions compared to the Lower Nile. Contrary to the Upper and Central Niles, negative trends are found for TWS variations over the Lower Nile.

- In addition to the trends, several strong impacts of precipitation, e.g., the 2007 ENSO rains, are also observed leading to strong rise and fall in both surface water storage and TWS variations time series.
- Large correlation coefficient between the precipitation and ENSO is found with an average of 0.67 indicating that precipitation and correspondingly surface water in the Nile Basin follows the global climate variability. ENSO had the highest correlation coefficients with the three variables over the Central and Upper Nile in comparison to IOD.

Acknowledgement

M. Khaki is grateful for the research grant of Curtin International Postgraduate Research Scholarships (CIPRS)/ORD Scholarship provided by Curtin University (Australia). This work is a TIGeR publication.

References

Aboulela, H. (2012); Contribution of Satellite Altimetry Data in the Environmental Geophysical Investigation of the Northern Egyptian Continental Margin. International Journal of Geosciences, Vol. 3 No. 3, pp. 431-442, http://dx.doi.org/10.4236/ijg.2012.33047.

Agrawal, A.G., Petersen, L.R. (2003); Human immunoglobulin as a treatment for West Nile virus infection. J Infect Dis 188, 14, http://dx.doi.org/10.1086/376871.

Ahmed, A.A., El Daw, A.K. (2004); An Overview on Cooperation of Trans-Boundary water: Case of the Nile River Basin, the 2nd Regional Arab water conf, Cairo, Egypt.

Ahmed, B.M., El Hussein, A.M., EL Khider, A.O. (2005); Some observations on ticks (Acari: Ixodidae) infesting sheep in River Nile Province of Northern Sudan. Onderstepoort Journal of Veterinary Research, 72:239243.

Ahmed, A.A., Ismail, U.A.E. (2008); Sediment in the Nile River System, Consultancy Study requested by UNESCO.

Ahmed, A.E., Roghim, S., Saleh, A. (2014); Poverty Determinants in South Sudan: The Case of Renk County, Asian Journal of Agricultural Extension, Economics & Sociology 4(2): 125-136, 2015; Article no. AJAEES.2015.013, ISSN: 23207027, http://dx.doi.org/10.9734/AJAEES/2015/12724.

Ahmed, M., Abdelmohsen, K. (2018); Quantifying Modern Recharge and Depletion Rates of the Nubian Aquifer in Egypt, Surv Geophys (2018) 39: 729. https://doi.org/10.1007/s10712-018-9465-3.

Alsdorf, D.E., Rodrguez, E., Lettenmaier, D.P. (2007); Measuring surface water from space, Rev. Geophys., 45, RG2002, http://dx.doi.org/10.1029/2006RG000197.

AMCEN (2011); Addressing climate change challenges in Africa: a practical guide towards sustainable development. African Ministerial Conference on Environment (AMCEN), Addis Ababa.

Awange, J.L., Sharifi, M.A., Ogonda, G. et al. (2008); The Falling Lake Victoria Water Level: GRACE, TRIMM and CHAMP Satellite Analysis of the Lake Basin. Water Resour Manage, 22: 775, http://dx.doi.org/10.1007/s11269-007-9191-y.

Awange, J.L., Forootan, E., Kusche, J., Kiema, J.B.K., Omondi, P.A.,Heck, B., Fleming, K., Ohanya, S.O., Gonalves, R.M. (2013a); Understanding the decline of water storage across the Ramser-Lake Naivasha using satellite-based methods, Advances in Water Resources, Volume 60, October 2013, Pages 7-23, ISSN 0309-1708, http://dx.doi.org/10.1016/j.advwatres.2013.07.002.

Awange, J.L., Anyah, R., Agola, N., Forootan, E., Omondi, P. (2013b); Potential impacts of climate and environmental change on the stored water of Lake Victoria Basin and economic implications, Water Resour. Res., 49, 81608173, http://dx.doi.org/10.1002/2013WR014350.

Awange, J.L., Gebremichael, M., Forootan, E., Wakbulcho, G., Anyah, R., Ferreira, V.G., Alemayehu, T. (2014a); Characterization of Ethiopian mega hydrogeological regimes using GRACE, TRMM and GLDAS datasets, Advances in Water Resources, Volume 74, December 2014, Pages 64-78, ISSN 0309-1708, http://dx.doi.org/10.1016/j.advwatres.2014.07.012.

Awange, J.L., Forootan, E., Kuhn, M., Kusche, J., Heck, B. (2014b); Water storage changes and climate variability within the Nile Basin between 2002 and 2011. Advances in Water Resources, 73:115, http://dx.doi.org/10.1016/j.advwatres.2014.06.010.

Awange, J.L., Ferreira, V.G., Forootan, E., Khandu, Andam-Akorful, S.A., Agutu, N.O. and He, X.F. (2016); Uncertainties in remotely sensed precipitation data over Africa. Int. J. Climatol., 36: 303323, http://dx.doi.org/10.1002/joc.4346.

Awulachew, S.B., Demissie, S.S., Hagos, F., Erkossa, T., Peden, D. (2012); Water management intervention analysis in the Nile Basin. In S. B. Awulachew, V. Smakhtin, D. Molden, & D. Peden (Eds.), The Nile River Basin: Water, agriculture, governance and livelihoods (pp. 292311). Oxon,UK: Routledge.

Ayana, E.K., Awulachew, Bekele, S. (2008); Comparison of irrigation performance based on management and cropping types. In Awulachew, Seleshi Bekele; Loulseged, Makonnen; Yilma, Aster Denekew (Comps.). Impact of irrigation on poverty and environment in Ethiopia: draft proceedings of the symposium and exhibition, Addis Ababa, Ethiopia, 27-29 November 2007. Colombo, Sri Lanka: International Water Management Institute (IWMI). pp.14-26.

Barnston, A.G., Livezey, R.E. (1987); Classification, seasonality, and persistence of low-frequency atmospheric circulation patterns. Mon. Weather Rev. 115: 10831126.

Becker, M., Lovel, W., Cazenave, A., Gntner, A., Crtaux, J.F. (2010); Recent Hydrological Behavior of the East African Great Lakes Region Inferred from GRACE, Satellite Altimetry and Rainfall Observations. Comptes Rendus Geoscience, http://dx.doi.org/10.1016/j.crte.2009.12.010.

Benada, J.R. (1997); PODAAC Merged GDR (TOPEX/POSEIDON) Generation B User's Handbook, Version 2.0. JPL D-11007. Pasadena: Jet Propulsion Laboratory, California Institute of Technology.

Berry, P.A.M., Garlick, J.D., Freeman, J.A., Mathers, E.L. (2005); Global Inland Water Monitoring from Multi-Mission Altimetery. Geophysical Research Letter 32: L16401, http://dx.doi.org/10.1029/2005GL022814.

Beyene, T., Lettenmaier, D.P., Kabat, P. (2010); Hydrologic impacts of climate change on the

Nile River Basin: implications of the 2007 IPCC scenarios. Climatic Change, Volume 100, Issue 34, pp 433461, https://doi.org/10.1007/s10584-009-9693-0

Birkett, C.M. (1995); The Contribution of TOPEX/POSEIDON to the Global Monitoring of Climatically Sensitive Lakes. Journal of Geophysical Research 25: 17925.

Birkett, C., Murtugudde, R., Allan, T. (1999); Indian Ocean climate event brings floods to East Africa's lakes and the Sudd Marsh. GRL, 26(8), pp.1031-1034.

Birkett, C.M., Mertes, L.A.K., Dunne, T., Costa, M.H., Jasinski, M.J. (2002); Surface Water Dynamics in the Amazon Basin: Application of Satellite Radar Altimetry. Journal of Geophysical Research 107, http://dx.doi.org/10.1029/2001JD000609.

Boergens, E., Dettmering, D., Schwatke, C., Seitz, F. (2016); Treating the Hooking Effect in Satellite Altimetry Data: A Case Study along the Mekong River and Its Tributaries. Remote Sens., 8, 91, http://dx.doi.org/10.3390/rs8020091.

Bonsor, H.C., Shamsudduha, M., Marchant, B.P., MacDonald, A.M., Taylor, R.G. (2018); Seasonal and Decadal Groundwater Changes in African Sedimentary Aquifers Estimated Using GRACE Products and LSMs. Remote Sens., 10, 904.

Brown, G.S. (1977); The Average Impulse Response of a Rough Surface and Its Applications. IEEE Transactions on Antennas and Propagation 25: 6774.

Calmant, S., Seyler, F., Cretaux, J.F. (2008); Monitoring Continental Surface Waters by Satellite Altimetry. Surveys in Geophysics 29, http://dx.doi.org/10.1007/s10712-008-9051-1.

Camberlin, P. (2009); Nile Basin Climates. Dumont, Henri J. The Nile: Origin, Environments, Limnology and Human Use, Springer, pp.307-333, Monographiae Biologicae.

Cretaux , J-F., Jelinski, W., Calmant, S.Kouraev, A., Vuglinski, V., Berg Nguyen, M., Gennero, M-C., Nino, F., Abarca Del Rio, R., Cazenave, A., Maisongrande, P. (2011); SOLS: A Lake database to monitor in Near Real Time water level and storage variations from remote sensing data, J. Adv. Space Res., http://dx.doi.org/10.1016/j.asr.2011.01.004.

Center for International Earth Science Information Network - CIESIN - Columbia University, and Centro Internacional de Agricultura Tropical - CIAT. (2005); Gridded Population of the

World, Version 3 (GPWv3): Population Density Grid. Palisades, NY: NASA Socioeconomic Data and Applications Center (SEDAC), http://dx.doi.org/10.7927/H4XK8CG2.

Center for International Earth Science Information Network - CIESIN - Columbia University. (2016); Gridded Population of the World, Version 4 (GPWv4): Population Density Adjusted to Match 2015 Revision UN WPP Country Totals. Palisades, NY: NASA Socioeconomic Data and Applications Center (SEDAC), http://dx.doi.org/10.7927/H4HX19NJ.

Center for International Earth Science Information Network - CIESIN Columbia University. (2016); Documentation for the Gridded Population of the World, Version 4 (GPWv4). Palisades NY: NASA Socioeconomic Data and Applications Center (SEDAC). http://dx.doi.org/10.7927/H4D50JX4.

Chen, J., Jegen-Kulcsar, M. (2007); The empirical mode decomposition (EMD) method in MT data processing. - In: Ritter, O., Brasse, H. (Eds.), - Protokoll zum 22. Kolloquium Elektromagnetische Tiefenforschung, 22. Kolloquium Elektromagnetische Tiefenforschung (Hotel Maxiky, Dn, Czech Republic 2007), pp. 6776.

Cheng, M.K., Tapley, B.D. (2004); Variations in the Earth's oblateness during the past 28 years. Journal of Geophysical Research, Solid Earth, 109, B09402. http://dx.doi.org/10.1029/2004JB003028.

Coe, M.T., Birkett, C.M. (2004); Calculation of river discharge and prediction of lake height from satellite radar altimetry: Example for the Lake Chad basin. Water Resour. Res., 40, W10205, http://dx.doi.org/10.1029/2003WR002543.

Conway, D. (2002); Extreme Rainfall Events and Lake Level Changes in East Africa: Recent Events and Historical Precedents. In E.O. Odada and D. O. Olago (eds.) The East African Great Lakes: Limnology, Palaeolimnology and Biodiversity. Advances in Global Change Research V. 12. Kluwer, Dordrecht. Pp. 63-92.

Conway, D. (2017); Water resources: future Nile river flows. Nature Climate Change, 7 (5). pp. 319-320. ISSN 1758-678X.

Davis, C.H. (1995); Growth of the Greenland Ice Sheet: A Performance Assessment of Altimeter Retracking Algorithms. IEEE Transactions on Geo-Science and Remote Sensing 33 (5): 1108-1116, http://dx.doi.org/10.1109/36.469474.

Davis, C. H. (1997); A Robust Threshold Retracking Algorithm for Measuring Ice-Sheet Surface Elevation Change from Satellite Radar Altimeters. IEEE Transactions on Geoscience and Remote Sensing 35 (4), http://dx.doi.org/10.1109/36.602540.

Dee, D. P., Uppala, S. M., Simmons, A. J., Berrisford, P., Poli, P., Kobayashi, S., Andrae, U., Balmaseda, M. A., Balsamo, G., Bauer, P., Bechtold, P., Beljaars, A. C. M., van de Berg, L., Bidlot, J., Bormann, N., Delsol, C., Dragani, R., Fuentes, M., Geer, A. J., Haimberger, L., Healy, S. B., Hersbach, H., Hlm, E. V., Isaksen, L., Kllberg, P., Khler, M., Matricardi, M., McNally, A. P., Monge-Sanz, B. M., Morcrette, J.-J., Park, B.-K., Peubey, C., de Rosnay, P., Tavolato, C., Thpaut, J.-N. and Vitart, F. (2011); The ERA-Interim reanalysis: configuration and performance of the data assimilation system. Q.J.R. Meteorol. Soc., 137: 553597, doi: 10.1002/qj.828.

Döll, P., Kaspar, F., Lehner, B. (2003); A global hydrological model for deriving water availability indicators: model tuning and validation, J Hydrol 207:105134.

Döll, P., Mller Schmied, H., Schuh, C., Portmann, F.T., Eicker, A. (2014); Global-scale assessment of groundwater depletion and related groundwater abstractions: Combining hydrological modeling with information from well observations and GRACE satellites, Water Resour. Res., 50, http://dx.doi.org/10.1002/2014WR015595.

Elshamy, M.E., Seierstad, I.A., Sorteberg, A. (2009); Impacts of climate change on Blue Nile flows using bias-corrected GCM scenarios, Hydrol. Earth Syst. Sci., 13, 551-565, http://dx.doi.org/10.5194/hess-13-551-2009.

FAO Land and Water Division. (1997); Irrigation potential in Africa; A basin approach. Food and Agriculture Organization of the United Nations, Rome (Italy).

Flandrin, P., Gonalvs, P., Rilling, G. (2004); Detrending and denoising with empirical mode decompositions, 12th European Signal Processing Conference, Vienna, 2004, pp. 1581-1584.

Forootan, E., Kusche, J. (2012); Separation of global time-variable gravity signals into maximally independent components, J Geod 86: 477, https://doi.org/10.1007/s00190-011-0532-5.

Forootan, E., Kusche, J. (2013); Separation of deterministic signals using independent component analysis (ICA), J. Stud Geophys Geod, 57: 17, https://doi.org/10.1007/s11200-012-0718-1.

Forootan, E., Rietbroek, R., Kusche, J., Sharifi, M. A., Awange, J., Schmidt, M., Omondi, P., Famiglietti, J. (2014); Separation of large scale water storage patterns over Iran using GRACE, altimetry and hydrological data. Journal of Remote Sensing of Environment, 140, 580-595, http://doi.org/10.1016/j.rse.2013.09.025.

Forootan, E., Khandu, Awange, J., Schumacher, M., Anyah, R., van Dijk, A., Kusche, J., (2016); Quantifying the impacts of ENSO and IOD on rain gauge and remotely sensed precipitation products over Australia. Remote Sensing of Environment,172, Pages 50-66, http://dx.doi.org/10.1016/j.rse.2015.10.027.

Frappart, F., Calmant, S., Cauhope, M., Seyler, F., Cazenave, A. (2006); Preliminary results of envisat ra-2-derived water levels validation over the amazon basin, Remote Sensing of Environment, 100(2), 252-264.

Frappart, F., Papa, F., Famiglietti, J.S., Prigent, C., Rossow, W.B., Seyler, F. (2008); Interannual variations of river water storage from a multiple satellite approach: A case study for the Rio Negro River basin. Journal of Geophysical Research, 113, D21104. doi:10.1029/2007JD009438.

Frappart, F. Papa, F., Gntner, A., Werth, S., da Silva, J.S., Tomasella, J., Seyler, F., Prigent, C., Rossow, W.B., Calmant, S., Bonnet, M.P. (2011); Satellite-based estimates of groundwater storage variations in large drainage basins with extensive floodplains, Remote Sensing of Environment, Volume 115, Issue 6, Pages 1588-1594, ISSN 0034-4257, https://doi.org/10.1016/j.rse.2011.02.003.

Fu, L.L., Christensen, E., Yamarone, C.A. (1994); TOPEX/POSEIDON mission overview. J. geophys. Res., 99, http://dx.doi.org/10.1029/94JC01761.

Goddard, L., Graham, N.E. (1999); Importance of the Indian Ocean for simulating rainfall anomalies over eastern and Southern Africa. J Geophys Res 104:19099.

Goita, K., Diepkile, A.T. (2012); Radar altimetry of water level variability in the Inner Delta of Niger River. IEEE, International Geoscience and Remote Sensing Symposium (IGARSS), Munich, Germany, 5262-5265, http://dx.doi.org/10.1109/IGARSS.2012.6352422.

Gomez-Enri, J., Vignudelli, S., Quartly, G., Gommenginger, C., Benveniste, J. (2009);

Bringing Satellite Radar Altimetry Closer to Shore. Remote Sensing, SPIE Newsroom, http://dx.doi.org/10.1117/2.1200908.1797.

Gruber, A., Dorigo, W.A., Crow, W., Wagner, W. (2017); Triple Collocation-Based Merging of Satellite Soil Moisture Retrievals, in IEEE Transactions on Geoscience and Remote Sensing, vol. 55, no. 12, pp. 6780-6792, doi: 10.1109/TGRS.2017.2734070.

Hassan, A.A., Jin, S. (2014); Lake level change and total water discharge in East Africa Rift Valley from satellite-based observations, In Global and Planetary Change, Volume 117, Pages 79-90, ISSN 0921-8181, https://doi.org/10.1016/j.gloplacha.2014.03.005.

Huang, N.E., Shen, Z., Long, S.R., Wu, M.C., Shih, H.H., et al. (1998); The empirical mode decomposition and the Hilbert spectrum for nonlinear and non-stationary time series analysis. Proceedings of the Royal Society of London A 454: 903-995.

Hwang, C.W., Kao, Y.H. (2010); A Preliminary Analysis of Lake Level and Water Storage Changes over Lakes Baikal and Balkhash from Satellite Altimetry and Gravimetry. Terrestrial, Atmospheric and Oceanic Sciences 22: 97108, http://dx.doi.org/10.3319/TAO.2010.05.19.01(TibXS).

Ismail, S.S., Samuel, M.G. (2011); Response of river Nile dredging on water levels. Fifteenth International Water Technology Conference, IWTC-15 2011, Alexandria, Egypt .

Khaki, M., Forootan, E., Sharifi, M.A. (2014); Satellite radar altimetry waveform retracking over the Caspian Sea. Int. J. Remote Sens., 35(17), 63296356, http://dx.doi.org/10.1080/01431161.2014.951741.

Khaki, M., Forootan, E., Sharifi, M.A., Awange, J., Kuhn, M. (2015); Improved gravity anomaly fields from retracked multimission satellite radar altimetry observations over the Persian Gulf and the Caspian Sea. Geophys. J. Int. 202 (3): 1522-1534, http://dx.doi.org/10.1093/gji/ggv240.

Khaki, M., Hoteit, I., Kuhn, M., Awange, J., Forootan, E., van Dijk, A.I.J.M., Schumacher, M., Pattiaratchi, C., (2017a). Assessing sequential data assimilation techniques for integrating GRACE data into a hydrological model, Advances in Water Resources, Volume 107, Pages 301-316, ISSN 0309-1708, http://dx.doi.org/10.1016/j.advwatres.2017.07.001.

Khaki, M., Schumacher, M., J., Forootan, Kuhn, M., Awange, E., van Dijk, A.I.J.M., (2017b). Accounting for Spatial Correlation Errors in the Assimilation of GRACE into Hydrological Models through localization, Advances in Water Resources, Available online 1 August 2017, ISSN 0309-1708, https://doi.org/10.1016/j.advwatres.2017.07.024.

Khaki, M., Ait-El-Fquih, B., Hoteit, I., Forootan, E., Awange, J., Kuhn, M., (2017c). A two-update ensemble Kalman filter for land hydrological data assimilation with an uncertain constraint, In Journal of Hydrology, Volume 555, 2017, Pages 447-462, ISSN 0022-1694, https://doi.org/10.1016/j.jhydrol.2017.10.032.

Khaki, M., Forootan, E., Kuhn, M., Awange, J., Papa, F., Shum, C.K., (2018a). A Study of Bangladesh's Sub-surface Water Storages Using Satellite Products and Data Assimilation Scheme, accepted in Advances in Water Resources.

Khaki, M., Forootan, E., Kuhn, M., Awange, J., van Dijk, A.I.J.M., Schumacher, M., Sharifi, M.A., (2018b). Determining Water Storage Depletion within Iran by Assimilating GRACE data into the W3RA Hydrological Model, Advances in Water Resources, 114:1-18,

Khaki, M., Forootan, E., Kuhn, M., Awange, J., Longuevergne, L., Wada, W., (2018c). Efficient Basin Scale Filtering of GRACE Satellite Products, In Remote Sensing of Environment, Volume 204, Pages 76-93, ISSN 0034-4257, https://doi.org/10.1016/j.rse.2017.10.040.

Khaki, M., Ait-El-Fquih, B., Hoteit, I., Forootan, E., Awange, J., Kuhn, M., (2018d). Unsupervised ensemble Kalman filtering with an uncertain constraint for land hydrological data assimilation, In Journal of Hydrology, Volume 564, Pages 175-190, ISSN 0022-1694, https://doi.org/10.1016/j.jhydrol.2018.06.080.

Khandu, Forootan, E., Schumacher, M., Awange, J.L., Mller Schmied, H. (2016); Exploring the influence of precipitation extremes and human water use on total water storage (TWS) changes in the Ganges-Brahmaputra-Meghna River Basin, Water Resour. Res., 52, 22402258, http://dx.doi.org/10.1002/2015WR018113.

Kizza, M., Rodhe, A., Xu, C.Y., Natle, K.H., Halldian, S., (2009); Temporal rainfall variability in the Lake Victoria Basin in east Africa during the twentieth century Theor. Appl. Climatol., 98, pp. 119-135.

Lee, H., Shum, C.K., Yi, Y., Ibaraki, M., Kim, J.W., Braun, A., Kuo, C.Y., Lu, Z. (2009); Louisiana Wetland Water Level Monitoring Using Retracked TOPEX/POSEIDON Altimetry. Marine Geodesy 32: 284302, http://dx.doi.org/10.1080/01490410903094767.

Lorenz, E. (1956); Empirical orthogonal function and statistical weather prediction. Technical Report Science Report No 1, Statistical Forecasting Project. MIT, Cambridge.

Lyon, B., Mason, S.J. (2007); The 199798 Summer Rainfall Season in Southern Africa. Part I: Observations. J. Climate, 20, 51345148, https://doi.org/10.1175/JCLI4225.1.

Martin, T.V., Zwally, H., Brenner, A.C., Bindschadler, R.A. (1983); Analysis and Retracking of Continental Ice Sheet Radar Altimeter Waveforms. Journal of Geophysical Research 88 (C3): 1608, http://dx.doi.org/10.1029/JC088iC03p01608.

Mayer-Gürr, T., Zehentner, N., Klinger, B., Kvas, A. (2014); ITSG-Grace2014: a new GRACE gravity field release computed in Graz. - in: GRACE Science Team Meeting (GSTM), Potsdam am: 29.09.2014.

Massachusetts Institute of Technology. (2017); Climate change predicted to increase Nile flow variability: Climate change could lead to overall increase in river flow, but more droughts and floods, study shows. ScienceDaily. Retrieved June 22, 2018 from www.sciencedaily.com/releases/2017/04/170424141236.htm.

McNally, A., Arsenault, K., Kumar, S., Shukla, S., Peterson, P., Wang, S., Funk, C., Peters-Lidard, C.D., Verdin, J.P. (2017); A land data assimilation system for sub-Saharan Africa food and water security applications. Scientific Data 4, Article number: 170012, http://dx.doi.org/10.1038/sdata.2017.12.

McSweeney, C., Lizcano, G., New, M., Lu, X. (2010); The UNDP climate change country profiles: improving the accessibility of observed and projected climate information for studies of climate change in developing countries. Bull Am Meteorol Soc 91:157166.

Mistry, V.V., Conway, D. (2003); Remote forcing of East African rainfall and relationships with fluctuations in levels of Lake Victoria. Int J Climatol 23(1):67.

Mohamed, Y.A., van den Hurk, B.J.J.M., Savenije, H.H.G., Bastiaanssen, W.G.M. (2005); Impact of the Sudd wetland on the Nile hydroclimatology, Water Resour. Res., 41, W08420, http://dx.doi.org/10.1029/2004WR003792.

Muala, E., Mohamed, Y.A., Duan, Z., van der Zaag, P. (2014); Estimation of Reservoir Discharges from Lake Nasser and Roseires Reservoir in the Nile Basin Using Satellite Altimetry and Imagery Data. Remote Sens., 6, 7522-7545.

Multsch, S., Elshamy, M.E., Batarseh, S., Seid, A.H., Frede, H.-G., Breuer, L. (2017); Improving irrigation efficiency will be insufficient to meet future water demand in the Nile Basin, Journal of Hydrology: Regional Studies, Volume 12, Pages 315-330, ISSN 2214-5818, https://doi.org/10.1016/j.ejrh.2017.04.007.

Nazemosadat, M.J., Cordery, I. (2000); On the relationships between ENSO and autumn rainfall in Iran. Int J Climatol 20:4761.

Nunzio, J. (2013); Conflict on the Nile: the future of transboundary water disputes over the world's longest river. Dalkeith: Future Directions International.

Nurutami, M.N., Hidayat, R. (2016); Influences of IOD and ENSO to Indonesian Rainfall Variability: Role of Atmosphere-ocean Interaction in the Indo-pacific Sector, Procedia Environmental Sciences, Volume 33, 2016, Pages 196-203, ISSN 1878-0296, http://dx.doi.org/10.1016/j.proenv.2016.03.070.

Omondi, P., Awange, J.L., Ogallo, L.A., Okoola, R.A., Forootan, E. (2012); Decadal rainfall variability modes in observed rainfall records over East Africa and their relations to historical sea surface temperature changes. Journal of Hydrology. 464-465: pp. 140-156.

Omondi, P., Awange, J.L., Ogallo, L.A., Ininda, J., Forootan, E. (2013); The influence of low frequency sea surface temperature modes on delineated decadal rainfall zones in Eastern Africa region. Advances in Water Resources. 54: pp. 161-180.

Papa, F., Durand, F., Rossow, W.B., Rahman, A., Bala, S. (2010); Satellite altimeter-derived monthly discharge of the Ganga-Brahmaputra River and its seasonal to interannual variations from 1993 to 2008. J. Geophys. Res., 115, C12013, http://dx.doi.org/10.1029/2009JC006075.

Papa, F., Frappart, F., Malbeteau, Y., Shamsudduha, M., Vuruputur, V., Sekhar, M., Ramillien, G., Prigent, C., Aires, F., Pandey, R.K., Bala, S., Calmant, S. (2015); Satellite-derived surface and sub-surface water storage in the GangesBrahmaputra River Basin, Journal of Hydrology: Regional Studies, Volume 4, Part A, September 2015, Pages 15-35, ISSN 2214-5818, http://dx.doi.org/10.1016/j.ejrh.2015.03.004.

Prigent, C., Matthews, E., Aires, F., Rossow, W.B. (2001); Remote sensing of global wetland dynamics with multiple satellite data sets, Geophys. Res. Lett., 28, 4631 4634, doi:10.1029/2001GL013263.

Prigent, C., Papa, F., Aires, F., Rossow, W.B., Matthews, E. (2007); Global inundation dynamics inferred from multiple satellite observations, 1993 2000, J. Geophys. Res., 112, D12107, doi:10.1029/2006JD007847.

Rao, S. A., Behara, S. K., Masumoto, Y., Yamagata, T. (2002); Interannual subsurface variability in the tropical Indian Ocean with a special emphasis on the Indian Ocean Dipole, Deep Sea Res., Part II, 49, 1549 1572.

Reynolds, R.W., Smith, T.M., Liu, C., Chelton, D.B., Casey, K.S., Schlax, M.G. (2007); Daily high-resolution blended analyses for sea surface temperature. J. Climate, 20, 5473-5496.

Rilling, G., Flandrin, P., Goncalves, P. (2003); On empirical mode decomposition and its algorithms. in: Proceedings IEEE-EURASIP Workshop on Nonlinear Signal and Image Processing NSIP-03, Grado I, p. 3.

Rogers, J. (1984); The Association between the North Atlantic Oscillation and the Southern Oscillation in the Northern Hemisphere. Mon. Wea. Rev., 112, 19992015, http://dx.doi.org/10.1175/1520-0493(1984)112¡1999:TABTNA¿2.0.CO;2.

Samuel, M.G. (2014); Limitations of navigation through Nubaria canal, Egypt. Journal of Advanced Research, 5, 147155, http://dx.doi.org/10.1016/j.jare.2013.01.006.

Sandwell, D.T. (1990); Geophysical Applications of Satellite Altimetry. Reviews of Geophysics Supplement, p. 132-137.

Schneider, U, Becker, A, Finger, P, Meyer-Christoffer, A, Rudolf, B, Ziese, M. (2015); GPCC Full Data Reanalysis Version 7.0 at 1.0: Monthly Land-Surface Precipitation from Rain-Gauges built on GTS-based and Historic Data, http://dx.doi.org/10.5676/DWD_GPCC/FD_M_V7_100.

Schumacher M., Eicker, A., Kusche, J., Schmied, H.M., Dll, P. (2015); Covariance Analysis and Sensitivity Studies for GRACE Assimilation into WGHM. In: Rizos C., Willis P. (eds) IAG 150 Years, International Association of Geodesy Symposia, vol 143. Springer, Cham.

Schwatke, C., Dettmering, D., Bosch, W., and Seitz, F. (2015); DAHITI an innovative approach for estimating water level time series over inland waters using multi-mission satellite altimetry, Hydrol. Earth Syst. Sci., 19, 4345-4364, http://dx.doi.org/10.5194/hess-19-4345-2015.

Seyler, F., Calmant, S., Santos da Silva, J., Filizola, N., Roux, E., Cochonneau, G., Vauchel, P., Bonnet, M.-P. (2008); Monitoring water level in large trans-boundary ungauged basins with altimetry: the example of ENVISAT over the Amazon basin. Journal of Applied Remote Sensing, 7150: 715017, http://dx.doi.org/10.1117/12.813258.

Siam, M.S., Eltahir, E.A.B. (2015); Explaining and forecasting interannual variability in the flow of the Nile River, Hydrol. Earth Syst. Sci., 19, 1181-1192, http://dx.doi.org/10.5194/hess-19-1181-2015.

Stoffelen, A. (1998); Toward the true near-surface wind speed: Error modeling and calibration using triple collocation, J. Geophys. Res., 103(C4), 77557766.

Sultan, M., Ahmed, M., Sturchio, N., Eugene, Y., Milewski, A., Becker, R., Wahr, J., Becker, D., Chouinard ,K. (2013); Assessment of the vulnerabilities of the Nubian sandstone fossil aquifer, North Africa, in (R. A. Pielke, Editor), Climate Vulnerability: Understanding and addressing threats to essential resources. Elsevier, 311-333 pp.

Swenson, S., Wahr, J. (2002); Methods for inferring regional surface-mass anomalies from Gravity Recovery and Climate Experiment (GRACE) measurements of time-variable gravity. Journal of Geophysical research, 107, B9, 2193. http://dx.doi.org/10.1029/2001JB000576.

Swenson, S., Wahr, J. (2006); Post-processing removal of correlated errors in GRACE data. Geophysical Research Letters, 33, L08402. http://dx.doi.org/10.1029/2005GL025285.

Swenson, S., Chambers, D., Wahr, J. (2008); Estimating geocentervariations from a combination of GRACE and ocean model output. Journal of Geophysical research, 113, B08410. http://dx.doi.org/10.1029/2007JB005338.

Swenson, S., Wahr, J. (2009); Monitoring the water balance of Lake Victoria, East Africa, from space, J. Hydrol., 370(14), 163176, http://dx.doi.org/10.1016/j.jhydrol.2009.03.008.

Taye, M.T., Ntegeka, V., Ogiramoi, N.P., Willems, P. (2011); Assessment of climate change impact on hydrological extremes in two source regions of the Nile River Basin, Hydrol. Earth Syst. Sci., 15, 209-222, http://dx.doi.org/10.5194/hess-15-209-2011.

Trenberth, K.E. (1990); Recent observed interdecadal climate changes in the Northern Hemisphere. Bull. Amer. Me- teor. Soc., 71,988-993.

Tropical Rainfall Measuring Mission (TRMM) (2011); TRMM (TMPA/3B43) Rainfall Estimate L3 1 month 0.25 degree x 0.25 degree V7, Greenbelt, MD, Goddard Earth Sciences Data and Information Services Center (GES DISC), Accessed [Data Access Date] https://disc.gsfc.nasa.gov/datacollection/TRMM_3B43_7.html.

Tseng, K.H., Shum, C.K. , Yi, Y., Fok, H.S., Kuo, C.Y., Lee, H., Cheng, X., Wang, X. (2013); Envisat Altimetry Radar Waveform Retracking of Quasi-Specular Echoes over the Ice-Covered Qinghai Lake. Terrestrial Atmospheric and Oceanic Science 24: 615627, http://dx.doi.org/10.3319/TAO.2012.12.03.01(TibXS).

Uebbing, B., Kusche, J., Forootan, E. (2015); Waveform retracking for improving level estimations from Topex/Poseidon, Jason-1 and -2 altimetry observations over African lakes, IEEE Trans. Geosci. Remote Sens., 53(4), 22112224.

Wahr, J.M., Molenaar, M., Bryan, F. (1998); Time variability of the Earth's gravity field: hydrological and oceanic effects and their possible detection using GRACE. J Geophys Res 108(B12):3020530229, http://dx.doi.org/10.1029/98JB02844.

Wingham, D.J., Rapley, C.G., Griffiths, H. (1986); New Techniques in Satellite Altimeter Tracking Systems, ESA Proceedings of the 1986 International Geoscience and Remote Sensing Symposium (IGARSS 86) on Remote Sensing. Todays Solutions for Tomorrows Information Needs 3: 13391344.

Woodward, J.C., Macklin, M.G., Krom, M.D., Williams, M.A.J. (2007); The Nile: evolution, Quaternary River Environments and material fluxes. In Large Rivers: Geomorphology and Management. Wiley, Chichester, 261-292.

Worley, S.J., Woodruff, S.D., Reynolds, R.W., Lubker, S.J., Lott, N. (2005); ICOADS Release 2.1 data and products. Int. J. Climatol. (CLIMAR-II Special Issue), 25, 823-842, http://dx.doi.org/10.1002/joc.1166.

Yang, L., Lin, M., Liu, Q., Pan, D. (2012); A Coastal Altimetry Retracking Strategy Based on Waveform Classification and Sub-Waveform Extraction. International Journal of Remote Sensing 33 (24): 78067819, http://dx.doi.org/10.1080/01431161.2012.701350.

Yilmaz, M.T.,Crow, W.T., Anderson, M.C., Hain, C.(2012); An objective methodology for merging satellite and modelbased soil moisture products, Water Resour. Res., 48, W11502, doi:10.1029/2011WR011682.

Yin, X., Nicholson, S.E. (1998); The water balance of Lake Victoria. Hydrol. Sci. J. Sci. Hydrol. 43 (5), 789811.

Zakharova, E., Kouraev, A., Cazenave, A. (2006); Amazon river discharge estimated from the Topex/Poseidon altimetry, C. R. Geosci., 338, 188196.

Zaroug, M.A.H., Eltahir, E.A.B., Giorgi, F. (2014); Droughts and floods over the upper catchment of the Blue Nile and their connections to the timing of El Nio and La Nia events, Hydrol. Earth Syst. Sci., 18, 1239-1249, http://dx.doi.org/10.5194/hess-18-1239-2014.